SUPPLEMENTARY MATERIAL

Microconstriction arrays for high-throughput quantitative measurements of cell mechanical properties

Janina R. Lange[1], Julian Steinwachs[1], Thorsten Kolb[1,3], Lena A. Lautscham[1], Irina Harder[2], Graeme Whyte[4,+], and Ben Fabry[1+]

[1]*Biophysics Group, Department of Physics, Friedrich-Alexander University of Erlangen-Nuremberg, 91052 Erlangen, Germany*

[2]*Max Planck Institute for the Science of Light, 91058 Erlangen, Germany*

[3]*Division of Molecular Genetics, German Cancer Research Center (DKFZ), 69120 Heidelberg, Germany*

[4]*IB3: Institute of Biological Chemistry, Biophysics and Bioengineering, Department of Physics, Heriot-Watt University, Edinburgh, UK*

[+] *Contributed equally*

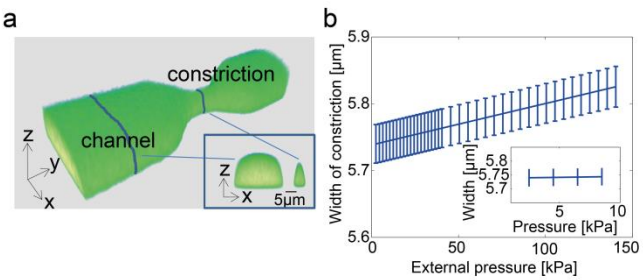

Fig. S1 Stability of microconstriction dimensions during pressure application:

The device is filled with fluorescein-dextran (FITC-dextran 70, Cat. No. 46945; Sigma-Aldrich), and the constrictions are imaged with a confocal microscope (SP5; Leica Microsystems) at a resolution of 0.2 µm × 0.2 µm × 0.5 µm during application of increasing pressures, ranging from 100 Pa to 150 kPa. **a**) 3D view of a constriction. Inset: cross-sections of the channel and the constriction. **b**) Constriction width versus externally applied pressure. Constriction dimensions increase only slightly with pressure. Error bars show standard deviations from 20 measurements evenly spaced along the length of the constriction. Inset shows a magnified view over the pressure range used in this study (0-10 kPa). Over this pressure range, no significant changes of constriction dimensions are observed.

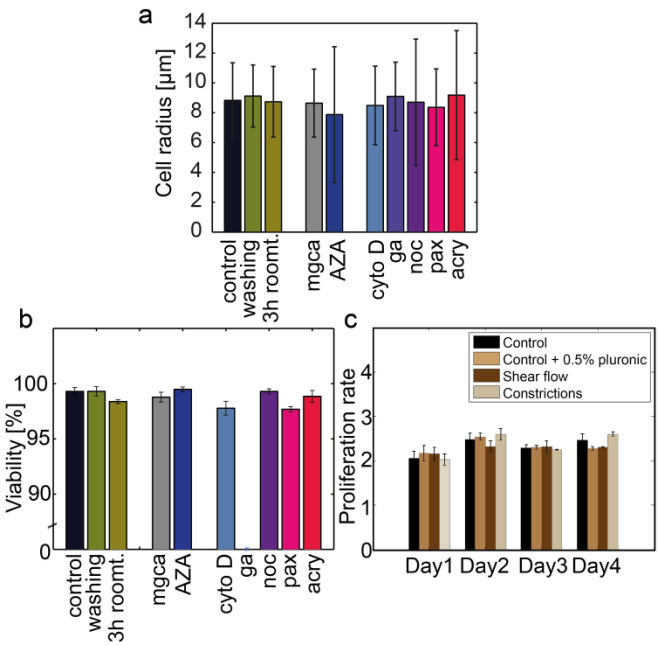

Fig. S2 Cell morphology, viability, and proliferation after chemical treatments or after passage through microconstrictions:

a) Radius of K562 cells is neither affected by treatment with different drugs (concentrations and incubation times as specified in Methods), nor by washing and centrifugation (4min at 1400rpm), nor by 3 h incubation at room temperature in normal cell medium (mean ± sd of n>10,000 cells per condition), demonstrating that the cell mechanical responses reported here are not caused by secondary cell radius changes. **b)** Cell viability of K562 cells is neither altered after drug treatments (concentrations as specified in Materials and Methods, incubation times all prolonged by 1 h), nor after the preparation procedure (washing, centrifugation for 4min at 1400rpm, resuspension), nor after 3 h incubation at room temperature. Cell viability is higher than 95% for all conditions except after treatment with glutaraldehyde. Error bars are standard deviations of 25 field-of-views with a total of n>10,000 cells for each condition. **c)** Proliferation rates over 4 days for cells during incubation in 1% pluronic, after the application of shear flow with a device consisting of a single 20 µm wide channel, and after passage through a microconstriction device without bypass. Cells are cultured in 96 well plates at an initial density of 250,000 cells/ml, and cell density is measured every 24 h with a Neubauer hemocytometer. The cell proliferation rate is calculated as the ratio of cell densities between consecutive days. Proliferation rates remain constant for all conditions and stable over time. Error bars are standard deviations from 8 measurements.

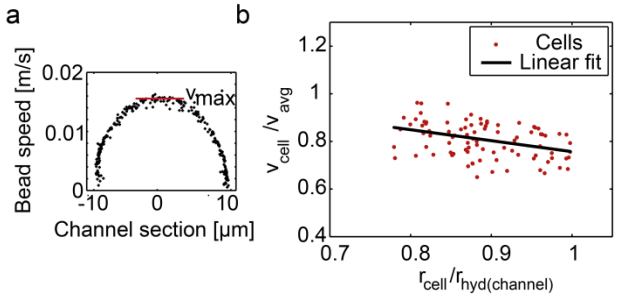

Fig. S3 Dependency of cell speed on average flow speed:

a) Velocity profile of a rectangular channel (x-y-profile, flow direction in y, h=17 µm, w=20 µm, focal plane at mid-section) measured by tracking polystyrene beads of 1 µm in diameter suspended in cell culture medium. From the maximum velocity v_{max} of the beads (red line), the average flow speed of the medium v_{avg} in a rectangular channel with $h \leq w$ can be approximated as $v_{avg} = 2/3 \cdot v_{max}$ (1). **b)** Dependency of relative cell speed v_{cell} / v_{avg} on the ratio of $r_{cell}/r_{(hyd)channel}$. The hydrodynamic radius of the channel $r_{(hyd)channel}$ is calculated as $r_{(hyd)channel} = (h \cdot w)/(h+w)$. Cells in our experiments ($r_{cell}/r_{(hyd)channel} > 0.7$) travel at lower speed than the average flow speed, and moreover the cell speed decreases with increasing cell radius. This can be approximated by a linear relationship according to $v_{cell} / v_{avg} = 1.22 - 0.46\ (r_{cell}/r_{(hyd)channel})$.

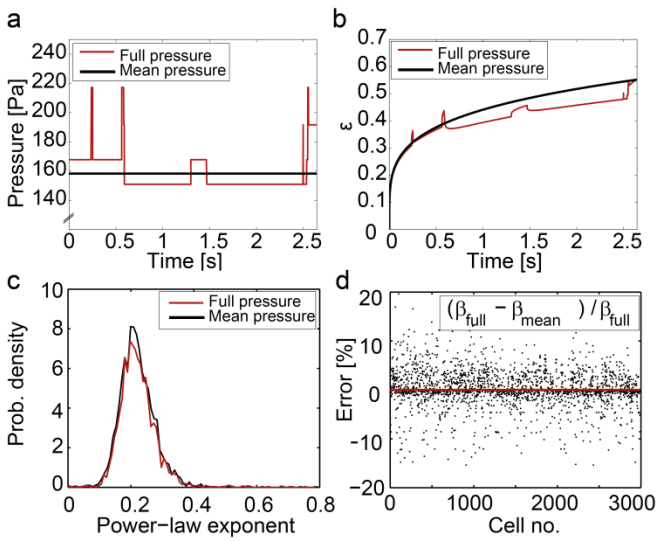

Fig. S4 Influence of driving pressure fluctuations on transit time:

a) Typical pressure fluctuations (red) across a microconstriction during cell transit. Pressure fluctuations are caused when cells enter or exit neighboring constrictions. Mean pressure is shown in black. **b**) Power-law deformation of a cell in a microconstriction versus time computed for a constant (mean) pressure according to Eq. 2 (black) and for the fluctuating pressure according to Boltzmann superposition (red). **c**) Distributions of the power-law exponent of

n=2984 cells under control conditions computed with Eq. 4 from the mean pressure transit time (β_{mean}, black) and the full pressure transit time (β_{full}, red). **d**) Relative error ($\delta\beta$ = 100(β_{full}- β_{mean})/β_{full}) of power-law exponents for n=2984 control cells (in %). The mean error of the power-law exponent $\langle\delta\beta\rangle$ approaches zero (-0.015%), indicating that the mean pressure approximation does not introduce a systematic error. The standard deviation of this error is 2.2%. Taken together, the mean pressure approximation for estimating cell mechanical properties with Eqs. 2 and 4 is unbiased and accurate for all practical purposes.

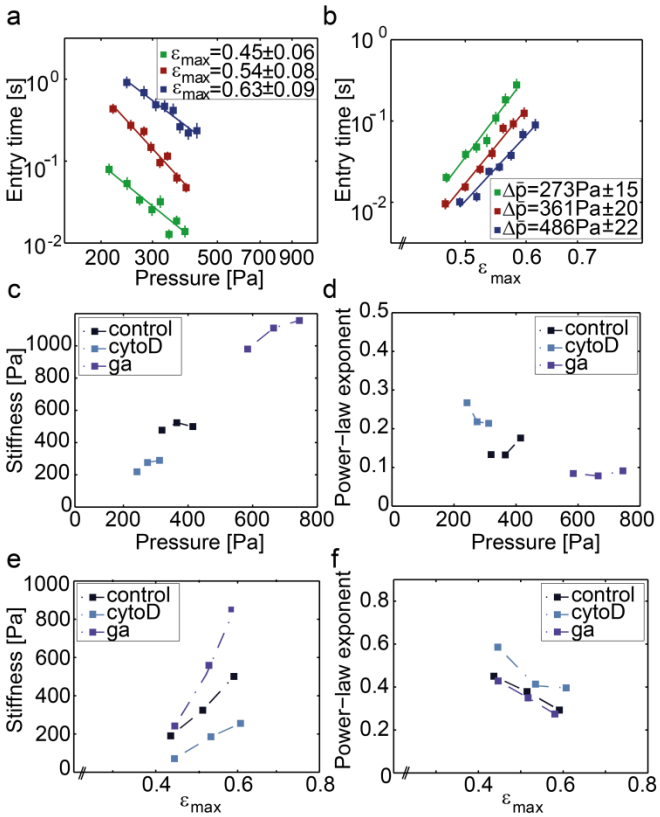

Fig. S5 Dependence of cell mechanical properties on pressure and maximum strain:

a) Power-law scaling of transit time versus pressure for cells with different maximum strain. Each marker represents the geometric mean ± geometric standard deviation of 80 cells with similar strain that are binned according to pressure. Lines are the fit of Eq. 3 to the binned data. **b**) Power-law scaling of transit time versus maximum strain for cells that have experienced different pressure ranges during transit. Each marker represents the geometric mean ± geometric standard deviation of 80 cells measured under different pressures that are binned according to maximum strain. Lines are the fit of Eq. 3 to the binned data. **c-f**) We also fit Eq. 3 to the data ($t_{entry}, \varepsilon_{max}, \Delta\bar{p}$) of selected cells (n~1000) that have experienced a similar pressure or strain. For each pressure or strain range, we obtain an average value for cell stiffness and fluidity. **c)** Cell stiffness versus working pressures for control cells and cells treated with cytochalasin D and glutaraldehyde. Cell stiffness is only slightly changed at different working pressures. **d**) The power-law exponent does not increase significantly with working pressures for different drug treatments. **e**) Cell stiffness increases significantly with maximum cell deformation particularly after glutaraldehyde treatment, indicating strain

stiffening. **f**) The power-law exponent does only slightly depend on maximum cell deformation for different drug treatments.

Taken together, the simplified assumption of pressure- and strain-independent cell mechanical properties is violated after glutaraldehyde treatment, but for all other drug treatments it is a reasonable approximation and is justified by the major simplification and numerical robustness for determining cell mechanical properties.

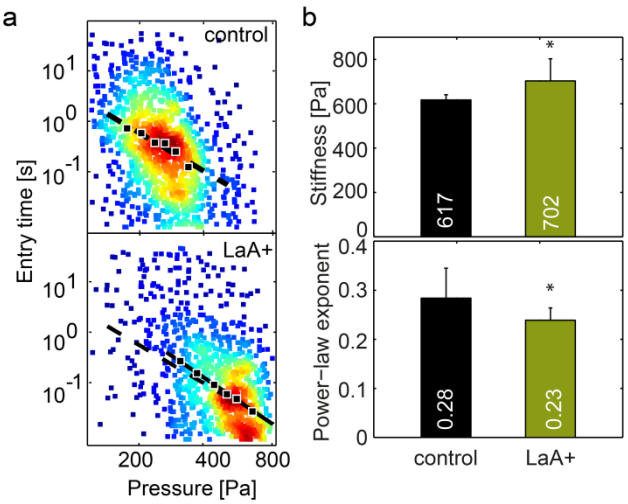

Fig. S6 Effect of lamin A-overexpression on adherent cells (epithelial breast carcinoma cells, MDA-MB-231):

As transfected cells are not FACS-sorted, we confirm a 2.3-fold increase of lamin A expression levels over control by Western blot analysis (data not shown). Adherent cells are trypsinized for 5 min before measurements and filtered with a cell strainer (pore size = 40 μm) to remove cell agglomerates. All measurements are completed within 40 min after trypsinization. **a**) Scatter plots of transit times versus applied pressure for control cells (top) and for GFP-lamin A transfected MDA-MB-231 cells (bottom). Black markers represent the geometric mean of approximately 500 cells binned according to pressure. Solid lines are the fit of Eq. 3 to the binned data. Fit to control data is shown for comparison in the LaA+ plot (dashed line). **b**) Population average of cell stiffness (top) and cell fluidity (bottom) for lamin A-overexpressing cells differ significantly ($p<0.0005$, indicated by asterisks) from control. Error bars represent standard deviations calculated by bootstrapping. These data are similar to our measurements on suspended K562 cells and demonstrate that our method can also be used to measure the mechanical properties of normally adherent cells.

Supporting references

1. Tanyeri, M., M. Ranka, N. Sittipolkul, and C.M. Schroeder. 2011. A microfluidic-based hydrodynamic trap: design and implementation. Lab Chip. 11: 1786–1794.